ORNL/SPR-2025/4216
M3LW-25OR0407015

Light Water Reactor Sustainability Program

Initial Characterization of Unirradiated Concrete and Summary of Stainless Steel Weld Harvesting from Ringhals Unit 2 in FY25

Samantha Sabatino
Xiang (Frank) Chen
Paula Bran Anleu
Lawrence Anovitz
Grant Helmreich
Michael Koehler
Adam Brooks
Mohammed Alnaggar
Yann Le Pape

September 2025

U.S. Department of Energy
Office of Nuclear Energy

ORNL/SPR-2025/4216
M3LW-25OR0407015

Initial Characterization of Unirradiated Concrete and Summary of Stainless Steel Weld Harvesting from Ringhals Unit 2 in FY25

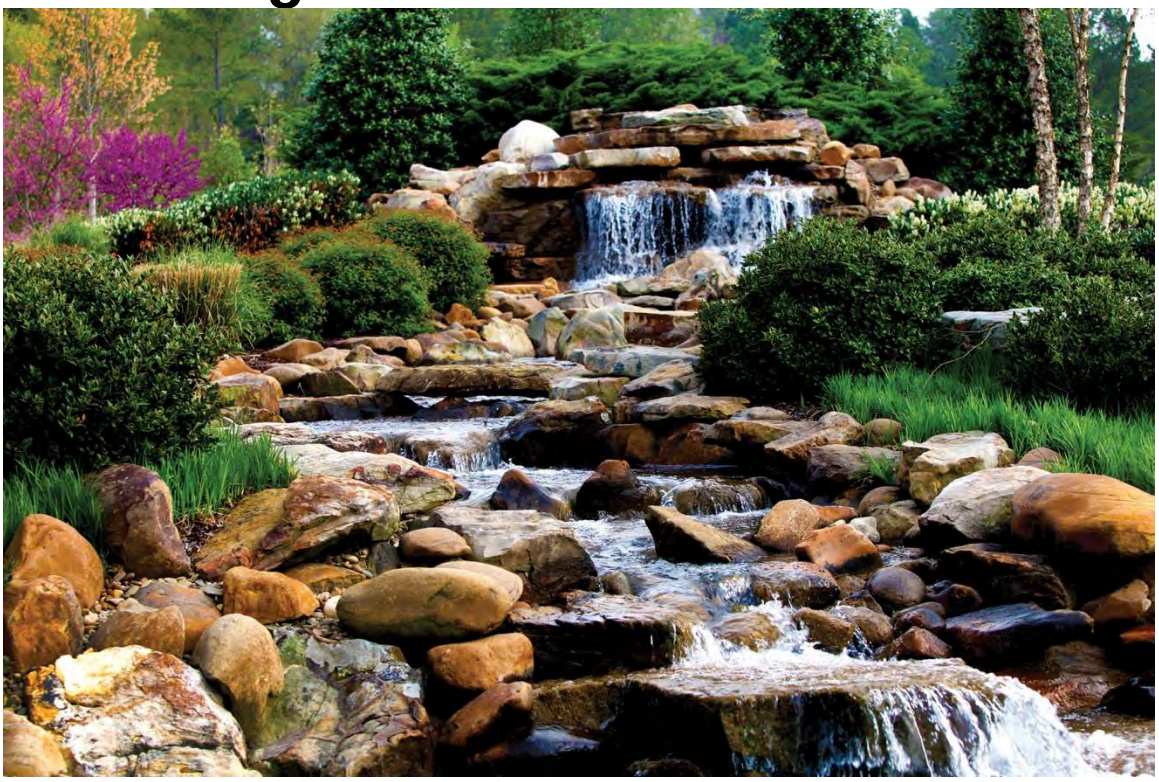

Samantha Sabatino
Xiang (Frank) Chen
Paula Bran Anleu
Lawrence Anovitz
Grant Helmreich
Michael Koehler
Adam Brooks
Mohammed Alnaggar
Yann Le Pape

September 2025

OAK RIDGE National Laboratory

ORNL IS MANAGED BY UT-BATTELLE LLC FOR THE US DEPARTMENT OF ENERGY

ORNL/SPR-2025/4216
M3LW-25OR0407015

Light Water Reactor Sustainability Program
Materials Research Pathway

Nuclear Energy and Fuel Cycle Division
Materials Science and Technology Division

INITIAL CHARACTERIZATION OF UNIRRADIATED CONCRETE AND SUMMARY OF STAINLESS STEEL WELD HARVESTING FROM RINGHALS UNIT 2 IN FY25

Samantha Sabatino
Xiang (Frank) Chen
Paula Bran Anleu
Lawrence Anovitz
Grant Helmreich
Michael Koehler
Adam Brooks
Mohammed Alnaggar
Yann Le Pape

September 2025

Prepared by
OAK RIDGE NATIONAL LABORATORY
Oak Ridge, TN 37831
managed by
UT-BATTELLE LLC
for the
US DEPARTMENT OF ENERGY
under contract DE-AC05-00OR22725

CONTENTS

LIST OF FIGURES

ABBREVIATIONS

Argonne	Argonne National Laboratory
CBS	concrete biological shield
CVR	Centrum výzkumu Řež
EDF	Électricité de France
EPRI	Electric Power Research Institute
IMAC	Irradiated Minerals, Aggregates, and Concrete
LWRS	Light Water Reactor Sustainability
NRC	US Nuclear Regulatory Commission
ORNL	Oak Ridge National Laboratory
PNNL	Pacific Northwest National Laboratory
RIVE	radiation-induced volumetric expansion
SEM	scanning electron microscopy
SONGS	San Onofre Nuclear Generating Station
XCT	x-ray computed tomography
XRD	x-ray diffraction
XRF	x-ray fluorescence

ACKNOWLEDGMENTS

This research was sponsored by the US Department of Energy Office of Nuclear Energy's Light Water Reactor Sustainability Program Materials Research Pathway under contract DE-AC05-00OR22725 with UT-Battelle, LLC/Oak Ridge National Laboratory (ORNL). The authors would like to kindly thank and acknowledge the help of Johanna Spåls and Pål Efsing from Vattenfall and Tom Rosseel from Imtech in the completion of this report.

EXECUTIVE SUMMARY

This report provides an in-depth study of the materials sourced from the Ringhals Nuclear Power Plant in Väröbacka, Sweden, documenting the characterization and analysis of reactor-grade concrete and stainless steel welds. These investigations, undertaken as part of a collaborative effort among Vattenfall, Oak Ridge National Laboratory (ORNL), the US Nuclear Regulatory Commission (NRC), the Electrical Power Research Institute (EPRI), and other international stakeholders, aim to deepen the understanding of material degradation mechanisms caused by prolonged exposure to high neutron fluence, gamma irradiation, elevated temperatures, thermal cycling, and corrosion environments in nuclear facilities. The initiative seeks to inform strategies for the sustainable operation, aging management, and decommissioning of nuclear power plants.

The history, operational framework, and decommissioning timeline of Ringhals Nuclear Power Plant Units 1 and 2 are important context for these studies. Unit 2's unirradiated concrete cores, with their distinctive silicate-rich aggregates containing quartz, feldspar, pyrite, garnet, amphibole, and other minerals, are being meticulously analyzed. Characterization techniques such as x-ray computed tomography (XCT), petrographic analysis, micro x-ray fluorescence (XRF), x-ray diffraction (XRD), and powder XRF enable researchers to quantify chemical and mineralogical structures, offering baseline data for comparative studies with irradiated samples. Initial findings reveal mineralogical heterogeneities and features such as pyrite inclusions and iron-rich phases. These observations highlight the importance of studying irradiation-induced effects, including phase transformations, oxidation, microcrack formation, and structural deterioration.

Stainless steel welds harvested from critical piping systems in Unit 2 provide additional opportunities to investigate aging-related degradation mechanisms. The welds are primarily composed of stainless steel alloy 316 and fabricated using gas tungsten arc welding and shielded metal arc welding methods, and they are susceptible to embrittlement, residual stress-induced crack initiation, and environmentally assisted fatigue. Collaborative efforts under the Light Water Reactor Sustainability Program facilitate characterization studies that include microstructural analysis and mechanical property testing to enhance the understanding of weld performance under extended operational conditions.

Key challenges such as the logistical complexities of irradiated material sampling, risk management in core extraction processes, and the need for international coordination are addressed in this report. The technical insights gained from the material characterization studies will improve predictive models of radiation-induced damage in reactor-grade concrete and stainless steel welds. Such improved models will benefit safety regulations, infrastructure aging management, and long-term operational strategies for nuclear facilities.

During FY 25, ORNL conducted the initial characterization of two unirradiated concrete cores from Ringhals Unit 2, utilizing advanced analytical techniques. These methods provided critical baseline information regarding the concrete's chemistry, mineralogy, and microstructural properties. XCT imaging revealed heterogeneities within the concrete, including distinct aggregate-matrix boundaries and internal void distributions, while micro XRF identified aggregate compositions dominated by silicate phases such as quartz and feldspar, along with iron-rich inclusions. XRD and petrography further confirmed the presence of accessory minerals, such as pyroxene and garnet, indicative of complex mineralogical features. These findings suggest the potential for oxidation, microcracking, and radiation-induced volumetric expansion (RIVE), which will be systematically evaluated in forthcoming studies involving irradiated specimens from Ringhals Unit 2's concrete biological shield (CBS). ORNL aims to leverage these findings to address critical knowledge gaps related to material behavior under irradiation and inform long-term strategies for nuclear infrastructure sustainability.

1. INTRODUCTION

The operational safety, long-term sustainability, and eventual decommissioning of nuclear power plants are critical aspects of global energy infrastructure. Prolonged exposure to radiation and extreme in-service conditions results in the degradation of structural materials, posing challenges to the reliability and integrity of nuclear reactor systems. This report explores the material characterization efforts stemming from the decommissioning of Ringhals Nuclear Power Plant's Unit 2. Comprehensive studies of reactor-grade concrete and stainless steel welds are being undertaken to provide vital insights into the aging behavior of materials under high-dose neutron fluence, gamma irradiation, and mechanically stressful environments. The overarching goal of the work is to advance materials science, inform regulatory frameworks, and optimize safety and operational efficiency in existing and future nuclear facilities.

The Ringhals Nuclear Power Plant, located in Väröbacka, Sweden, was commissioned with four reactors, one boiling water reactor (Unit 1) and three pressurized water reactors (Units 2, 3, and 4). Units 1 and 2 were shut down in 2019 and 2020 as part of an operational transition, and dismantling began in 2025. Unit 2 experienced extensive radiation exposure throughout its service life and therefore serves as a unique source of reactor-grade concrete and stainless steel welds for material degradation research. These materials exhibit key attributes, including gradients in spatial radiation doses and operational stress factors, that make them particularly valuable for assessing long-term performance under nuclear reactor conditions.

Unirradiated concrete cores from Unit 2, composed of silicate-rich aggregates such as quartz, feldspar, pyroxene, and biotite, provide opportunities for studying radiation-induced changes. Moreover, stainless steel welds extracted from piping systems enable investigations into microstructural changes and crack propagation mechanisms under thermal and mechanical conditions typical of reactor environments. Together, these materials provide a fuller perspective on aging processes that affect both metallic and non-metallic reactor components.

The primary objective of this initiative is to characterize unirradiated and irradiated materials from Ringhals Unit 2 and to evaluate the degradation mechanisms associated with prolonged radiation exposure and operational stress. Key goals include:

- Understanding radiation-induced damage in reactor-grade concrete aggregates, emphasizing chemical and phase transformations, crack initiation and propagation, and its influence on structural integrity.
- Investigating environmental effects, thermal aging, and fatigue-related damage in stainless steel welds, focusing on heat-affected zones and residual stress concentrations.
- Enhancing predictive models for material behavior by bridging data gaps in existing databases, such as the Irradiated Minerals, Aggregates, and Concrete (IMAC) database.
- Informing regulatory approaches for extended reactor life cycles, decommissioning, and aging management in nuclear facilities.

This report is organized as follows. Section 2 provides an overview of the Ringhals Nuclear Power Plant, including a summary of its operational history, the decommissioning timeline for Units 1 and 2, and the extraction of materials used as part of these studies. It also discusses radiation transport simulations and their relevance to sampling irradiated materials. Section 3 details the initial characterization efforts performed on the unirradiated concrete cores extracted from Unit 2. Advanced characterization techniques such as XCT, XRF, XRD, and petrographic analysis are described, along with key results that establish baseline properties of the concrete for comparison with irradiated samples. Section 4 focuses on stainless steel welds harvested from the plant's critical systems. It outlines the characterization efforts,

including analyses of thermal aging, environmentally assisted fatigue, and crack initiation mechanisms. It also describes the collaborative research framework under which these analyses are being carried out. Finally, Section 5 provides conclusions, summarizes the key findings, addresses remaining research challenges, and discusses the broader significance of these studies for the sustainable operation and decommissioning of nuclear facilities.

2. OVERVIEW OF RINGHALS NUCLEAR POWER PLANT

2.1 GENERAL PLANT INFORMATION

The Ringhals Nuclear Power Plant, located in Väröbacka, Sweden, was originally designed with four reactors: one boiling water reactor (i.e., Unit 1) alongside three pressurized water reactors (i.e., Units 2, 3, and 4). As of today, only Units 3 and 4 remain operational, as Units 1 and 2 were permanently shut down in 2019 and 2020, respectively. The facility is jointly owned by Vattenfall, which holds a 70% stake, and Uniper SE, which owns the remaining 30%. Ringhals continues to play a pivotal role in Sweden's nuclear energy production framework.

Unit 2 was commissioned in 1975 and remained in operation for over 43 years. The reactor's construction involved the use of concrete composed of aggregates with distinctive mineralogical properties specific to the region's geological characteristics. Historical records and preliminary concrete mix designs preserved by Vattenfall document the inclusion of coarse silicate-rich aggregates, likely incorporating metamorphic and igneous rocks such as pyroxene, quartz, and feldspar [1,2].

In late 2024, Vattenfall provided ORNL with two unirradiated concrete cores extracted from Unit 2. This material transfer was part of a collaborative effort between Vattenfall and ORNL to assess and benchmark the long-term effects of neutron and gamma irradiation on reactor-grade concrete. In addition, Vattenfall has extended an opportunity to access and harvest stainless steel welds from critical components of Ringhals Unit 2, including the surge, residual heat removal, and safety injection lines. These weld materials provide a rare and valuable opportunity for the study of degradation mechanisms in stainless steel welds after prolonged in-service exposure. This research is particularly relevant and timely, as similar degradation phenomena have been implicated in the recent weld failures observed across a substantial portion of the French Électricité de France (EDF) pressurized water reactor fleet. These failures have led to reduced electricity generation and considerable economic repercussions associated with extended reactor outages for inspection and repair.

Most of the welds available originate from components fabricated using gas tungsten arc welding and shielded metal arc welding processes on stainless steel 316. The opportunity to investigate these welds has garnered strong interest from key stakeholders, including ORNL, the NRC, and EPRI, all of whom aim to utilize these samples for further research and analysis. This initiative has the potential to advance the understanding of long-term weld performance in nuclear power plant environments and inform strategies to mitigate similar issues in existing reactor fleets globally.

2.2 DECOMMISSIONING TIMELINE

The decommissioning of Ringhals Units 1 and 2 is currently being overseen by Vattenfall, with technical contributions from Westinghouse Electric Company, which is handling the segmentation of the reactor pressure vessel (RPV), and from Nuvia, which is responsible for on-site dismantling activities. Physical dismantling operations commenced in 2025 and are anticipated to take approximately 8–10 years to complete. The full restoration of the site is projected to occur around 2033 [3].

Radiation transport simulations for the CBS of Unit 2 have been finalized by Vattenfall. The results demonstrate that the fluence threshold of 1×10^{19} n/cm^2 ($E > 0.1$ MeV) is surpassed up to a depth of 5 cm within the concrete. Additionally, gamma radiation doses in these regions have been estimated to reach approximately 70% of the established 100 MGy limit. These findings indicate moderate to significant irradiation effects in proximity to the inner surface of the CBS wall, rendering Unit 2 an exceptional case for investigating gradients in spatial radiation-induced damage [1].

The extraction of concrete cores from irradiated CBS sections, encompassing both high-dose and low-dose exposure zones, has been identified as a viable task within the outlined decommissioning timeframe. Effective planning is critical to synchronize coring operations with ongoing demolition activities and established safety protocols, ensuring the success and safety of these investigations.

2.3 ORNL INVOLVEMENT

2.3.1 FY 2025 Accomplishments

In FY 2025, ORNL finalized the initial characterization of two unirradiated concrete cores provided from Ringhals Unit 2. This comprehensive evaluation encompassed several key activities aimed at analyzing the internal structure and compositional features of the materials. XCT was employed to examine the internal morphology of the concrete, revealing aggregate distributions and material heterogeneities within the samples. Thin and polished sections were subsequently prepared for petrographic analysis, with five cross sections processed by Precision Petrographics.

Further analyses involved the targeted extraction of aggregates using a combination of heat and acid treatments. Detailed characterization of these aggregates was performed using multiple techniques. Micro XRF mapping identified that the majority of the aggregates were predominantly composed of quartz (30%–38%) and feldspar, with mineral inclusions of pyroxene and pyrite. Petrographic investigations corroborated the presence of biotite, amphibole, garnet, hematite, and pyroxene, features indicative of altered metamorphic rock origins. Powder XRF and XRD analyses provided additional semi-quantitative data, highlighting that quartz and feldspar dominated the mineralogical composition, while trace amounts of iron oxides and accessory minerals, such as cerium and vanadium, were also present.

The findings from this detailed characterization underscore the presence of pyrite inclusions and other iron-rich minerals within multiple aggregates. These observations raise important questions regarding the potential for radiation-induced degradation of such mineral phases. Particular concerns include the oxidation behavior of these minerals under irradiation, the potential onset of microcracking, and the formation of secondary minerals as a result of radiation exposure.

ORNL was also involved with the harvesting of a stainless steel weld. By collaborating with Vattenfall, NRC, and EPRI, ORNL identified the stainless steel 316 weld from the Ringhals Unit 2 surge line and initiated subcontracting with Studsvik, Vattenfall’s sole authorized subcontractor for metal harvesting, to harvest the weld.

2.4 PLANNED NEXT STEPS

2.4.1 Finalization of Unirradiated Concrete Characterization

Efforts to conclude the characterization of unirradiated concrete samples from Ringhals Unit 2 are currently underway. This process focuses on comprehensive mineralogical analysis to understand the intrinsic properties of the concrete aggregates. Specifically, automated mineralogical analyses of five aggregates are being conducted using scanning electron microscopy (SEM) coupled with energy-dispersive x-ray spectroscopy. This advanced technique offers precise spatial quantification of mineral content, providing a detailed understanding of the aggregates' composition and distribution. Such insights are essential for evaluating the concrete’s susceptibility to radiation-induced damage under the conditions experienced at Unit 2.

To predict potential degradation mechanisms, the observed mineralogical data will be compared with the limited dataset available in the IMAC database. While the IMAC database offers valuable insight into the

radiation-induced volumetric expansion (RIVE) behavior of irradiated minerals, its limited coverage, particularly regarding quartz, highlights the critical need for irradiated concrete samples to bridge these data gaps. The acquisition and characterization of such samples will ultimately enhance the predictive models for radiation-induced damage in nuclear-grade concrete.

2.4.2 Development of the Coring and Sampling Plan for Irradiated Concrete

A robust sampling strategy for the extraction of irradiated concrete from the CBS in Unit 2 is in development to address the challenges posed by both technical and logistical factors. The choice of coring locations will be guided by fluence maps and thermal history records to ensure comprehensive coverage of zones with varying irradiation levels. Particularly important are areas at mid-core elevations, which experience the highest neutron fluence, and regions with lower irradiation but comparable thermal environments, such as areas near the reactor pressure vessel (RPV) supports or adjacent to the cold and hot legs.

Delays could become significant if coring is postponed until after the RPV is removed. Coring from within the reactor cavity after RPV removal presents a number of complications. Ground-penetrating radar scanning, typically used to avoid rebar during drilling, is likely to be impaired due to the lined nature of the CBS. Additionally, performing core extraction inside the cavity will incur increased costs, primarily due to the need for scaffolding and the heightened radiation exposure in the active zone, which creates elevated risks for radiation workers.

The risks associated with drilling through rebar also necessitate careful planning. Even when the size and spacing of the rebar are known, calculating the steel-to-concrete ratio at the rebar plane cannot entirely eliminate the risk of encountering rebar. The primary concern lies not in retrieving steel fragments but in the risk of core breakage during drilling, which could prevent successful concrete extraction. To mitigate this, multiple cores are recommended in a given area, spaced approximately 0.5 meters apart to ensure recovery success.

The detailed sampling plan will also benefit from lessons learned from prior projects, such as the San Onofre Nuclear Generating Station (SONGS), and will integrate various coring strategies to address cost feasibility and technical reliability [4]. Following core extraction, the specimens will undergo a series of evaluations, including microstructural analysis, mechanical testing, and comparative assessments against unirradiated baseline properties.

2.4.3 Coordination and Responsibilities for Sample Handling

The handling and analysis of core samples will require careful coordination among all stakeholders, including Vattenfall, ORNL, Centrum výzkumu Řež (CVR), and researchers in Tokyo. Vattenfall will provide key technical resources, including detailed engineering drawings, concrete mix design data, and radiation transport simulation outputs. In addition, Vattenfall will facilitate on-site coring operations and conduct preliminary radiological screening of the samples.

ORNL will oversee advanced material testing, employing techniques such as XCT, XRF, XRD, and petrographic examinations, as well as detailed analysis of mineral composition using SEM. Handling of the irradiated materials, including their receipt, storage, and further analysis, will also be managed by ORNL. To support the project financially, funding is being pursued through the LWRS program and other aligned research initiatives.

The shipment and distribution of core samples among participating institutions will require additional deliberations. For example, mechanical disk tests may be conducted effectively and at lower costs at

CVR, while characterization techniques such as Raman spectroscopy or micro XRF mapping would be more suitable for ORNL's facilities. Additionally, discussions among technical collaborators are essential to finalize decisions regarding whether to ship the cores intact or segment them on-site at Ringhals, depending on the sample activation levels and the analytical capabilities of each institution.

2.4.4 Challenges and Recommendations for Coring Operations

Coring operations must resolve several outstanding challenges to ensure high-quality sample recovery. Consistency in core diameter across all samples is regarded as essential for downstream analyses. For instance, Raman scanning along the radial direction has been emphasized for measuring amorphization degrees and their correlation to RIVE. Similarly, mechanical evaluations, such as controlled disk-splitting tests, benefit from sufficiently large core diameters.

Given the cost and technical implications of core recovery, a variety of coring plans should be evaluated, each factoring in logistical constraints, safety measures, and the scientific requirements of subsequent analysis. To refine these strategies, the organization of a technical brainstorming workshop has been proposed involving key contributors, including ORNL, CVR, Tokyo, NRC, and Vattenfall. This workshop aims to align the roles of each participating organization, optimize technical workflows, and allocate tasks based on the specific expertise and resources of each partner.

With the overarching goal of advancing the scientific understanding of radiation effects on nuclear concrete, international collaboration remains pivotal. The expertise and contributions of each entity will be crucial in addressing both immediate logistical challenges and long-term research objectives.

2.4.5 Finalization of Characterization of Stainless Steel Weld

To complete the characterization of the stainless steel weld, the following actions are proposed:

- **Subcontract with Studsvik:** Establish an additional subcontract with Studsvik to facilitate the shipment of the harvested stainless steel welds to ORNL.
- **Research Collaboration:** Distribute the weld samples to multiple US national laboratories, including ORNL, Argonne National Laboratory (Argonne), and Pacific Northwest National Laboratory (PNNL). Under the coordination of the LWRS program, these laboratories will jointly investigate key aspects of weld performance, such as thermal aging effects, stress corrosion crack initiation and growth, and environmentally assisted fatigue behavior.
- **Return Shipment to Vattenfall:** Following the completion of characterization studies, the weld samples will be returned to Vattenfall in compliance with Swedish legal requirements.

This coordinated effort will enable a comprehensive understanding of the degradation mechanisms in stainless steel welds after long-term service exposure.

2.5 SIGNIFICANCE OF THE OPPORTUNITY

This research takes advantage of a rare opportunity to study concrete and stainless steel welds harvested from a reactor’s CBS and critical piping systems, offering valuable insights into how these materials age in nuclear environments. The concrete samples come from sections of the CBS with well-documented neutron and gamma dose gradients, making them ideal for analyzing radiation damage in silicate-rich aggregates. Of particular interest are the aggregates containing quartz and pyroxene, as well as reactive minerals like pyrite, which are prone RIVE. Studying the effects of irradiation on this particular concrete is especially important as RIVE and associated microstructural changes can severely impact the structural integrity of reactor-grade concrete.

The research focuses on three key goals: identifying how radiation induces phase changes and microstructural alterations, determining how cracks initiate and grow under varying radiation doses, and measuring changes in mechanical, physical, and chemical properties through comparisons between irradiated and unirradiated material. By establishing clear relationships between radiation exposure and material degradation, this work will support predictive models for assessing the long-term durability of biological shields in operating reactors.

At the same time, the project examines stainless steel welds harvested from the plant's piping systems. These welds, composed primarily of stainless steel 316, are critical structural components that have operated in high-temperature, thermally cycled, and corrosive environments for decades. The study investigates how these conditions drive microstructural changes such as precipitation hardening, embrittlement, and surface oxidation. Understanding these degradation mechanisms is essential to evaluating the long-term integrity of reactor components.

When analyzed together, the concrete and steel data will provide a comprehensive understanding of how radiation and reactor conditions affect key materials. The findings will play an important role in supporting aging management strategies, evaluating safety and structural performance over time, and informing decisions about inspection intervals, repairs, or decommissioning. The significance of this work lies in the rarity of the materials being studied (i.e., concrete and welds) with well-documented operational and irradiation histories. This unprecedented access allows researchers to better understand long-term radiation effects on reactor components and generate data critical to supporting the safe and efficient operation of nuclear facilities worldwide.

3. INITIAL CHARACTERIZATION OF UNIRRADIATED CONCRETE FROM RINGHALS UNIT 2

This section presents a comprehensive analysis of unirradiated concrete cores extracted from Unit 2 of the Ringhals Nuclear Power Plant, which serves as the baseline for understanding the material properties and behavior of nuclear-grade concrete prior to irradiation. This detailed investigation incorporates a variety of advanced characterization techniques, including XCT, XRF, XRD, petrographic analysis, and powder XRF. These methodologies enable researchers to examine the physical, chemical, and mineralogical properties of the concrete's aggregates and matrix at multiple scales, from macroscopic features to microstructural and elemental details.

The unirradiated concrete cores were subjected to XCT imaging to assess internal heterogeneities, material distributions, aggregate-matrix boundaries, and potential defects. The data obtained were processed to evaluate the concrete's overall morphology, including aggregate densities, voids, and spatial distribution. Following imaging, the cores were segmented into slices, which were further analyzed using micro XRF to generate high-resolution elemental maps. These maps revealed compositional information for the primary elements, supporting the identification of silicate minerals, feldspars, and other structural components. Additionally, detailed petrographic examinations were conducted on thin sections prepared from the concrete slices and individual aggregates, offering visual insights into the mineral phases, their geometry, and textural relationships.

Aggregate-specific characterization, which is critical to understanding the role of mineralogy in long-term concrete durability, included various preparatory steps designed to ensure minimal alteration during extraction and analysis. Various thermal, mechanical, and chemical treatments were used to isolate coarse aggregates from the cement matrix with sufficient fidelity. The extracted aggregates were then analyzed through an array of techniques. XRD and Rietveld refinement were applied to assess phase composition, while elemental analysis was conducted using powder XRF to determine the chemical makeup and distribution of metallic and non-metallic elements. Insights from these analyses were used to establish correlations between the mineralogical content and physical properties of the aggregates.

This section establishes the baseline dataset for the unirradiated concrete from Ringhals Unit 2, which will serve as a critical reference for understanding how neutron and gamma irradiation impact reactor-grade concrete. The dataset includes detailed measurements of void fraction, aggregate size distribution, and the quality of the aggregate–paste interface. High-resolution elemental maps from micro XRF illustrate the distribution of major elements within the concrete. Petrographic analysis documents key mineral phases, textures, and microstructural features, while XRD quantifies phase weight percentages with reliable fit statistics. Oxide totals determined from powder XRF provide additional insights into chemical composition. These baseline measurements will enable meaningful comparisons with irradiated samples, support dose–response analyses, and contribute to predictive models of mechanical performance and long-term durability. By quantifying the concrete's initial properties, this dataset provides the foundation for evaluating how exposure to radiation alters the material, with direct applications for aging management, safety assessments, and licensing decisions.

3.1 EXPERIMENTAL SETUPS FOR UNIRRADIATED CONCRETE CHARACTERIZATION

Vattenfall provided two cores of unirradiated concrete from Unit 2 of Ringhals nuclear power plant in Väröbacka, Sweden (Figure 1). The cores are approximately 7 cm in diameter and 12 and 8 cm tall, respectively.

Figure 1. Unirradiated concrete cores from Ringhals Nuclear Power Plant. The smaller core was used to extract aggregates, and the taller core was sliced for analysis after running an XCT scan.

3.1.1 XCT of Concrete Cores

The smaller core underwent a heat treatment to extract undamaged aggregates, and the larger core was imaged using a Zeiss Versa 620 with the source operating at 100 kV and 14 W. The source to rotation axis distance was 206 mm, and the rotation axis to detector distance was 60 mm, resulting in a final voxel size of 57.927 µm per pixel using the flat panel detector. A total of 3,201 radiographs were collected with a 1 s exposure time; they were then reconstructed into a 3D image using the default Zeiss reconstruction software based on filtered back projection.

After the XCT scan was completed, the core was sliced into eight slices of about 1 cm thick each (Figure 2). The slices were then separated for either micro XRF or petrography sample preparation (thin sections). Figure 3 shows the polished concrete surfaces for micro XRF. Thin sections were prepared (Figure 4), but they have not yet been analyzed. Instead, thin sections of the aggregates were analyzed (see Section 3.1.3).

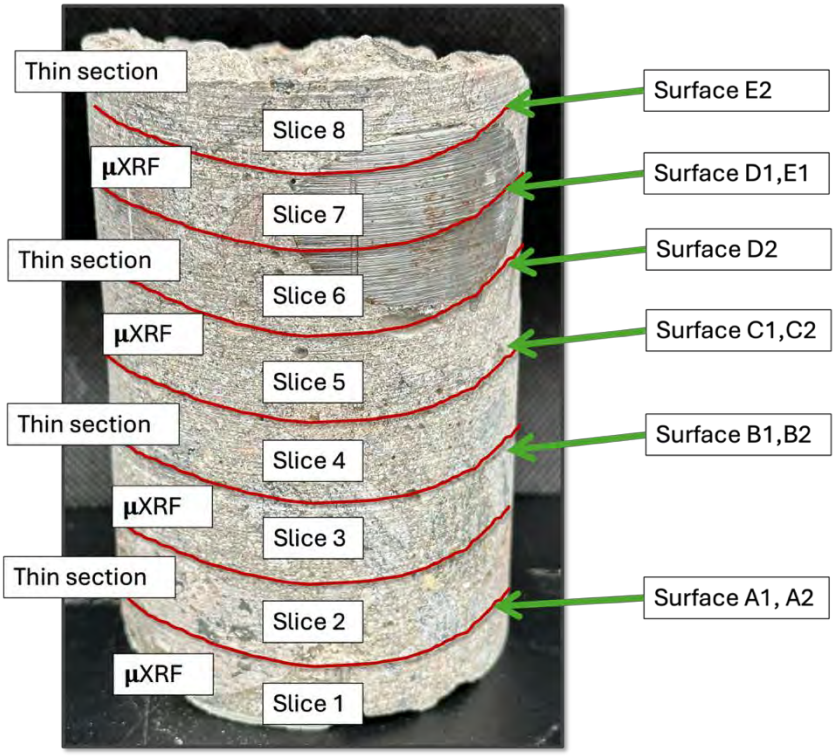

Figure 2. Schematic of the slices, surfaces, and procedures for the larger core.

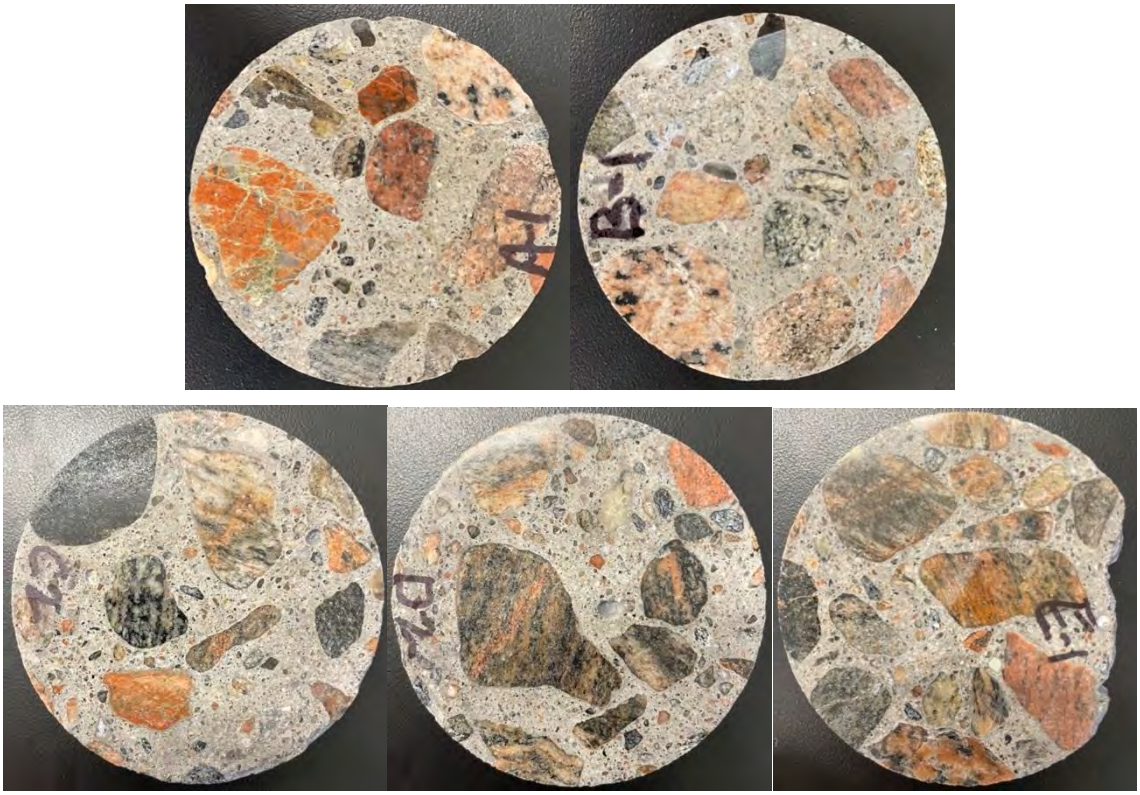

Figure 3. Polished concrete slices for micro XRF analysis.

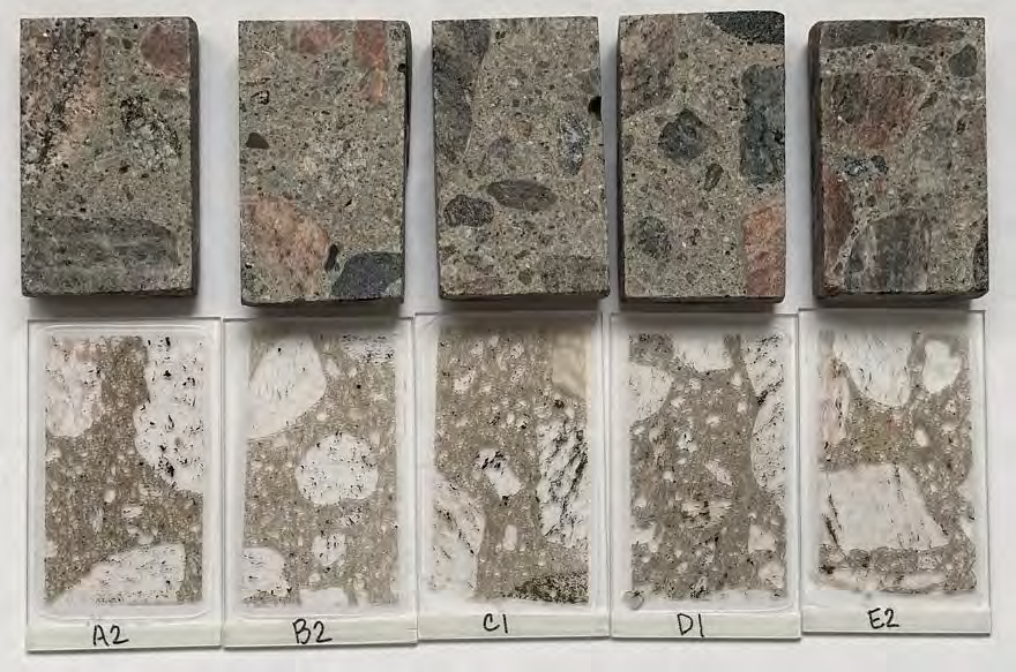

Figure 4. Polished sections (top) and thin sections (bottom) of the selected concrete cross sections.

3.1.2 Micro XRF of Concrete Slices

Micro XRF elemental maps were collected on surfaces A1, B1, C2, D2, and E1 using an Atlas system (IXRF Systems) operated under vacuum at 50 kV and 600 µA with a spot size of 10 µm. The map dimensions were 45 × 45 mm with a resolution of 1,500 pixels and a pixel size of 30 µm. Data were recorded for 300 ms, and the time constant was 2. Seven elements (i.e., aluminum, calcium, iron, potassium, manganese, sulfur, and silicon) were analyzed for consistency throughout the core.

3.1.3 Aggregates Preparation

To facilitate the analysis of aggregates, they had to be extracted from the mortar. Thus, various methodologies for aggregate extraction were examined. These methodologies are well-established in the field and are commonly employed in the processing of recycled concrete aggregates.

A literature review conducted for a previous characterization procedure (i.e., for SONGS) indicated that exposure to high temperatures ranging from 300°C to 500°C appears to have minimal adverse effects on aggregates; however, it significantly affects the cement matrix [4]. The degradation of concrete following exposure to elevated temperatures is attributed to changes in microstructure, characterized by increased total pore volume, leading to a reduction in compressive strength. Additionally, various chemical methods are employed in practice. After confirming the small presence of carbonates in the aggregates via micro XRF analysis, a combination of heat treatment, rigorous mechanical treatment, and chemical treatment was applied.

Core 2 underwent a series of three heat treatment cycles. It was rapidly heated to a temperature of 400°C and then quenched to room temperature in a series of three per cycle. The pieces were then hammered to separate the aggregates from the paste as much as possible. The residual mortar on the surface of the coarse aggregates was then dissolved by immersing the aggregates in HCl at room temperature. This acid treatment effectively dissolved the cement paste while minimizing damage to the aggregates.

The clean coarse aggregates confirm that the core contained a macroscopically homogeneous group of aggregates, exhibiting consistent texture and visible characteristics, while any mineralogical heterogeneity is analyzed and discussed at the microscopic level later in the text. Visually, aggregates are of similar shapes and colors, with few exceptions (Figure 5). The initial sorting was performed based on the color and texture (Figure 6). Five aggregates were cut, embedded in epoxy, and polished for micro XRF and quantitative evaluation of minerals by scanning electron microscopy mineralogical analysis. They were also cut into thin sections for petrography analyses (Figure 7). The remaining specimens were ground to fine powder for structural and chemical analyses using XRD and powder XRF.

Figure 5. Extracted aggregates from Core 2.

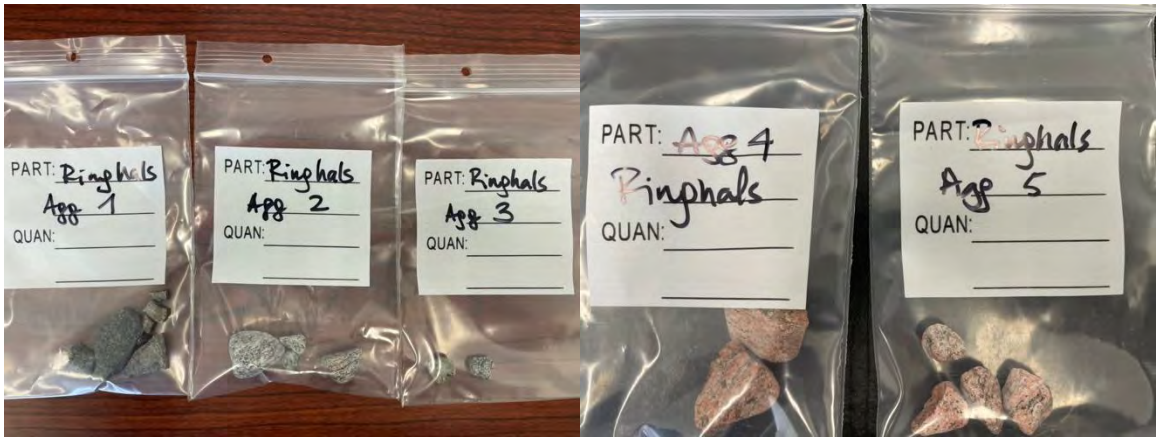

Figure 6. Selected aggregates for detailed characterization.

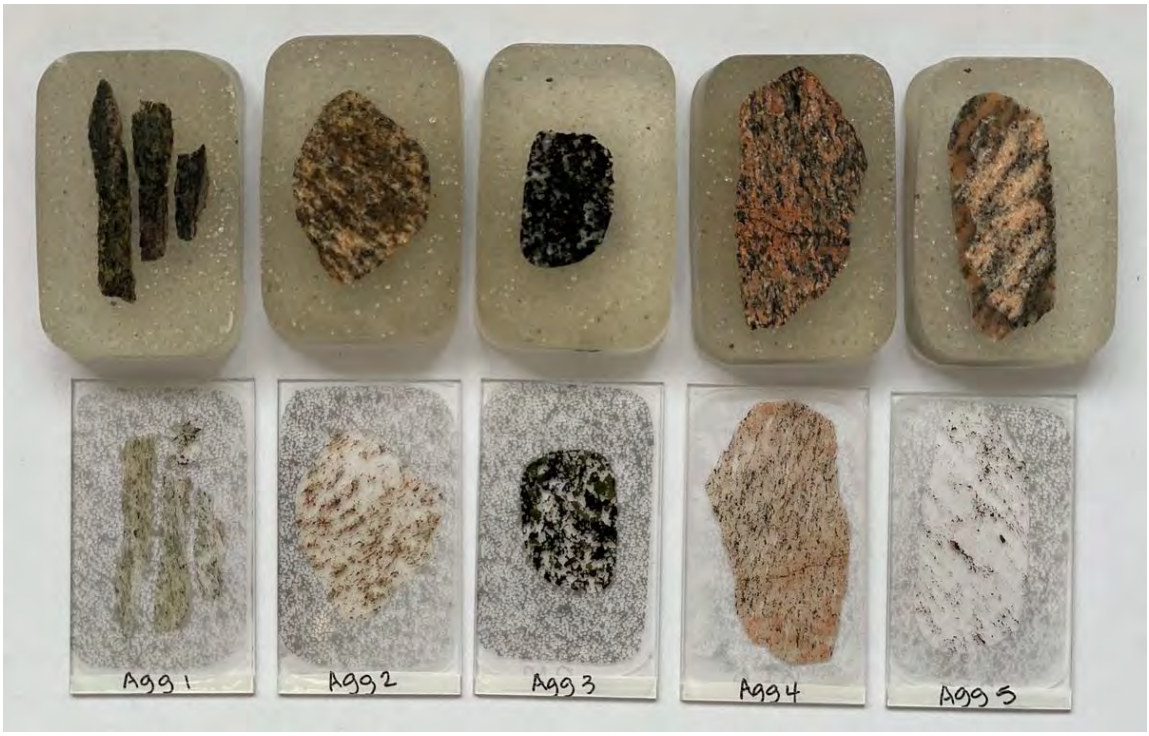

Figure 7. Polished sections and thin sections of the selected aggregates.

3.1.4 Petrography Analysis of Aggregates

Petrographic images of the thin sections were taken to qualitatively assess the mineral phases present in the aggregates. The work was performed using a Nikon D700 camera attached to an Olympus BX60 optical microscope. Images were taken at magnifications from 5× to 20× under transmitted light with crossed and uncrossed polarizers and under reflected light.

3.1.5 Micro XRF of Aggregates

Micro XRF maps were collected using an Atlas unit (IXRF Systems) operated at 50 kV and 600 µA. Data acquisition was performed under vacuum with a dwell time of 300 ms, a time constant of 2, a pixel size of 15 µm, and a resolution of 400 pixels. An area of 6 × 6 mm was mapped for every aggregate.

3.1.6 XRD of Aggregates

Data were collected with an Empyrean diffractometer (Cu-Kα x-rays) from Malvern Panalytical using a real-time sample stage. Incident beam optics for the Empyrean included a 7 mm automatic divergence slit, 10 mm mask, 4° antiscatter slit, and 0.04 radian Soller slit. The diffracted beam optics included a 7.0 mm automatic antiscatter slit, 0.04 radian Soller slits, a nickel filter, and a PIXcel3D detector in scanning line detector (1D) mode. The automatic divergent and antiscatter slits open as the experiment progresses to maintain the programmed beam length. The relative intensity differences caused by these automatic slits compared with standard fixed slits are corrected in HighScore Plus. The scan parameters included a 2θ range of 5°–100°, 0.0131° step size, 63 s/step, and a sample rotation speed of 4 s/revolution.

3.1.7 Powder XRF of Aggregates

XRF was performed on an Epsilon 1 system from Malvern Panalytical with a silver x-ray source. A small quantity of powder was placed in a sample holder that used a 3.6 μm Mylar film as its base. For each sample, four spectra were collected with various voltage and current settings as well as filters to optimize detection of different types of elements (each sample had identical settings for each individual spectrum). The results were normalized to approximately 100%.

3.2 RESULTS AND DISCUSSION OF UNIRRADIATED CONCRETE CHARACTERIZATION

3.2.1 XCT of Concrete Cores

The XCT image (Figure 8) shows distinct internal heterogeneities with varying false color intensities that correspond to different components of the concrete core. The brighter regions are interpreted as the coarse aggregates because of their higher density and x-ray attenuation; the bright yellow are dense inclusions. The surrounding matrix corresponds to hydrated cement paste, lower density aggregates, and voids.

The presence of distinct aggregate–matrix boundaries suggests a good resolution and phase contrast in the scan. The XCT imaging provides valuable insight into the internal morphology of the concrete, enabling qualitative assessments of aggregate distribution, voids and potential defects, and the uniformity of the matrix. Further quantitative image processing, including segmentation or porosity analysis, could provide more information such as volume fraction, aggregate to matrix ratio, and crack density.

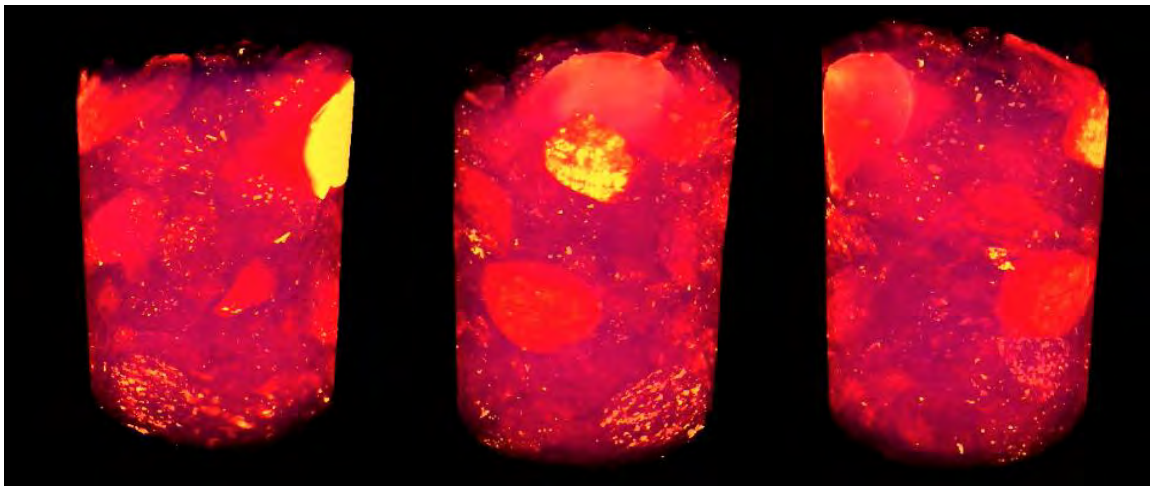

Figure 8. XCT scan to visualize (heavy) aggregates of interest. The very bright solid yellow at the top is a piece of reinforcement.

3.2.2 Micro XRF of Concrete Slices

The elemental maps of the concrete slices shown in Figure 9 and Figure 10 were obtained via micro XRF. These images show that most of the aggregates are primarily composed of potassium, silicon, and aluminum, indicating the presence of feldspars and silicates like quartz. However, some aggregates contain a higher iron content than most others and appear to have elevated levels of calcium. A clear illustration of this can be observed in Slice C2 (Figure 9) and some aggregates in Slice D2 (Figure 10), specifically in the dark aggregate located in the top right corner of the mapped area. Additionally, some aggregates exhibit europium inclusions.

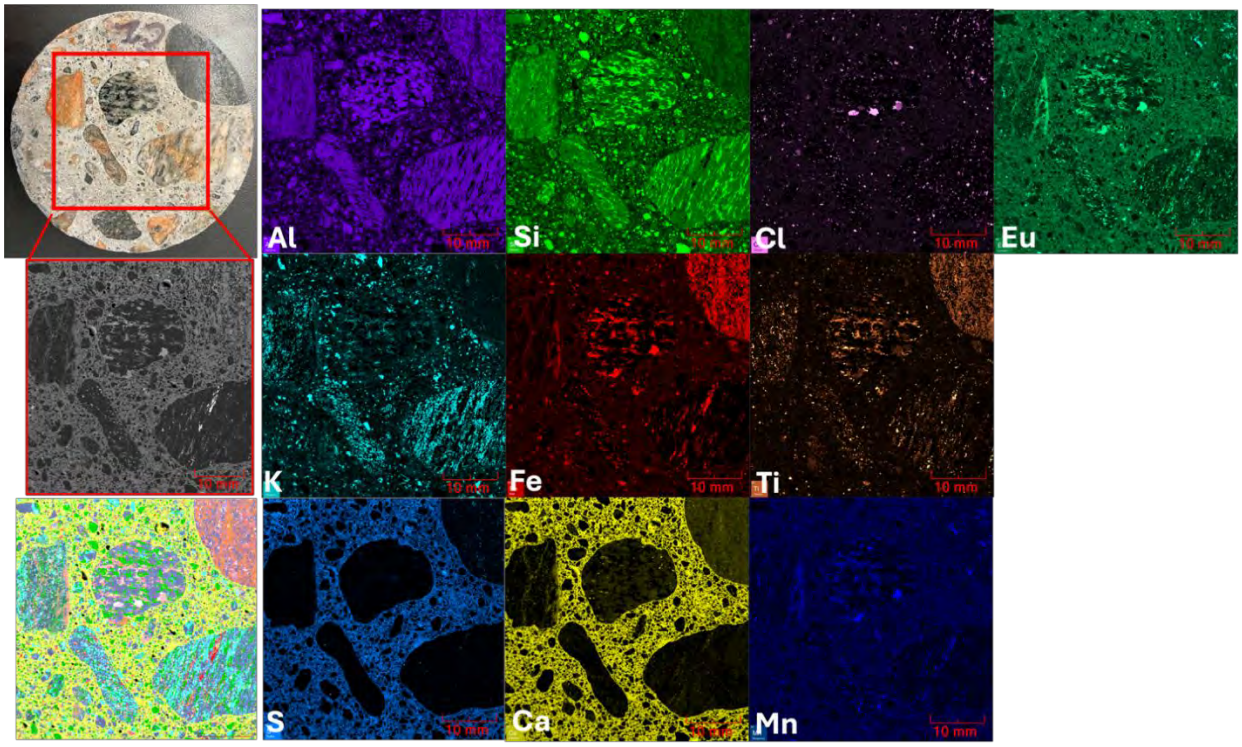

Figure 9. Elemental maps in concrete Slice C2. The image in the bottom left corner is a composite of the elemental maps shown in the figure.

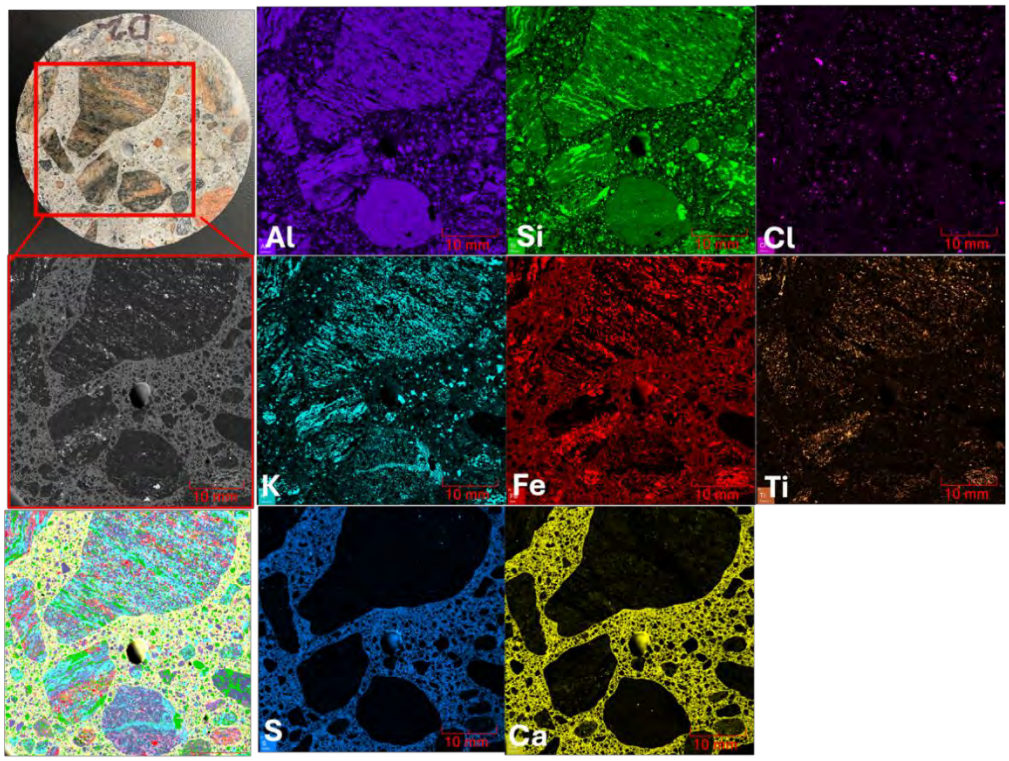

Figure 10. Elemental maps in concrete Slice D2. The image in the bottom left corner is a composite of the elemental maps shown in the figure.

3.2.3 Micro XRF of Aggregates

The elemental maps for the major elements present in the aggregates were obtained with micro XRF. Herein, the results for Aggregates 1 and 2 are presented in Figure 11 and Figure 12, respectively; Aggregates 4 and 5 are very similar to Aggregate 2, and Aggregate 3 is quite similar to Aggregate 1. Aggregate 1 (Figure 11) is a flat, dark gray to black aggregate resembling shale or schist. The chemical maps reveal a somewhat layered structure: aluminum, calcium, and potassium are the predominant elements. Aggregates 2 (Figure 12) and 5 (not presented in this report) are likely granitic in nature. They exhibit a clear layered structure characterized by the presence of iron, aluminum, titanium, and silicon. Aggregates 1 and 3 contain lower amounts of potassium and calcium compared with Aggregates 2 and 5. Aggregate 4 is probably another form of granite, but in contrast to Aggregates 2 and 5, it presents a more granular structure.

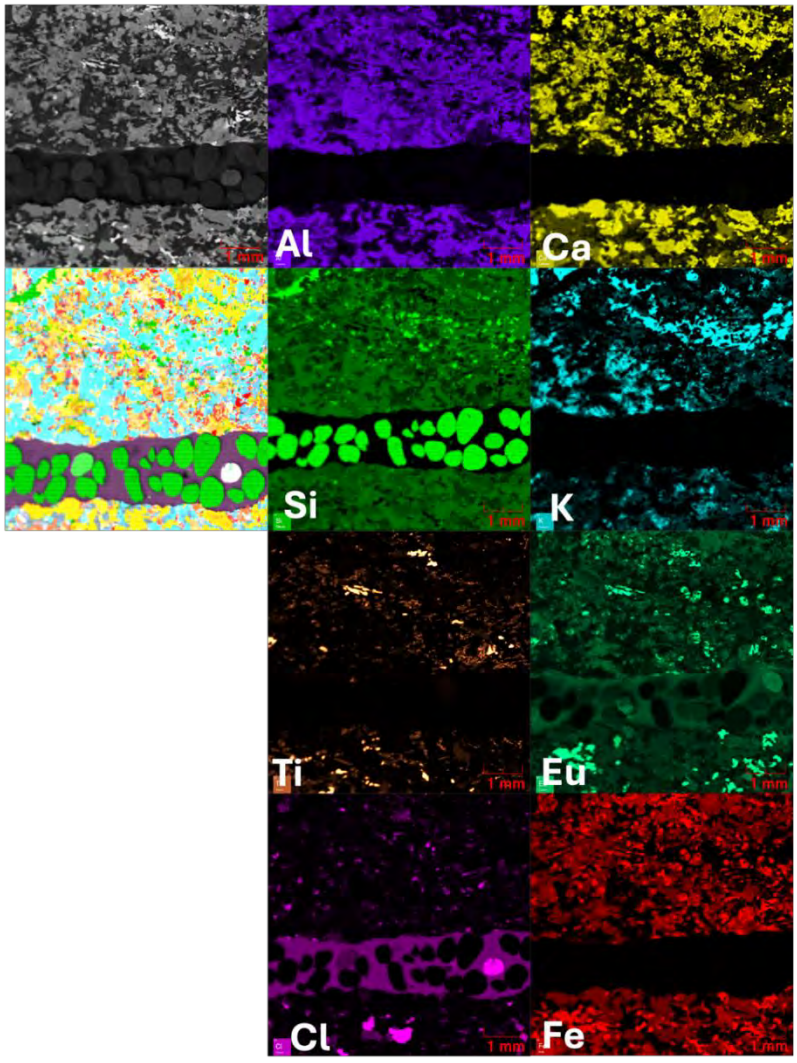

Figure 11. Elemental maps in Aggregate 1. The image in the second row, first column is a composite of the elemental maps shown in the figure.

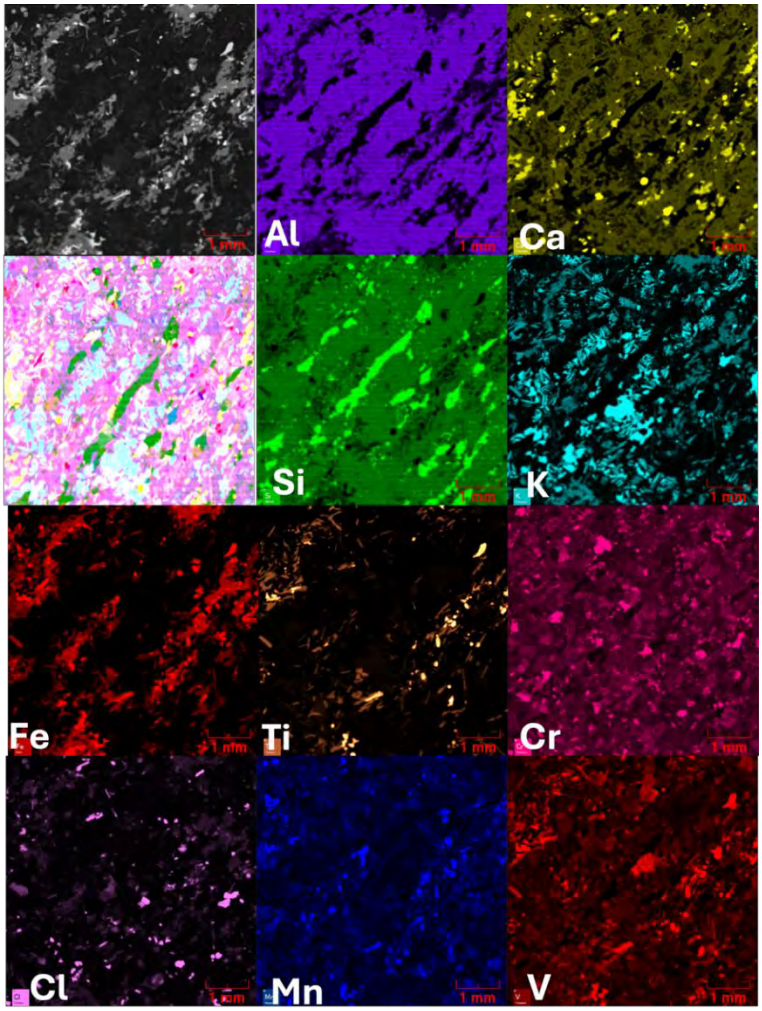

Figure 12. Elemental maps in Aggregate 2. The image in the second row, first column is a composite of the elemental maps shown in the figure.

3.2.4 Petrography of Aggregates

The results of the exploration of aggregates in the thin sections indicate a variety of altered metamorphic rocks. The following predominant minerals among the five aggregates were identified (in no particular order):

- Quartz
- Feldspars (altered and unaltered)
- Plagioclase feldspar
- Biotite
- Amphibole
- Epidote
- Iron oxides: hematite and possibly ilmenite
- Pyrite (altered and unaltered)
- Pyroxene
- Garnet
- Magnetite

Aggregate 1 exhibits significant alteration and is rich in garnet, biotite, and pyroxene (Figure 13). Alterations are noted in the lower right corner of the studied area in Figure 13, where pyrite is visible with the reflected light. The greenish mineral observed under polarized light may be epidote, and a vein in the structure contains quartz along with a preexisting layer of unknown origin. At a magnification of 5×, the presence of this turquoise material is pronounced; the black areas observed in crossed polarized light indicate garnet, which stays black when rotated at a 45° angle, indicating isotropy (Figure 14). The birefringent mineral shares similar characteristics to the rest of the sample, suggesting it may have fractured and subsequently reformed. Further analysis shows other minerals such as amphibole and hematite–ilmenite.

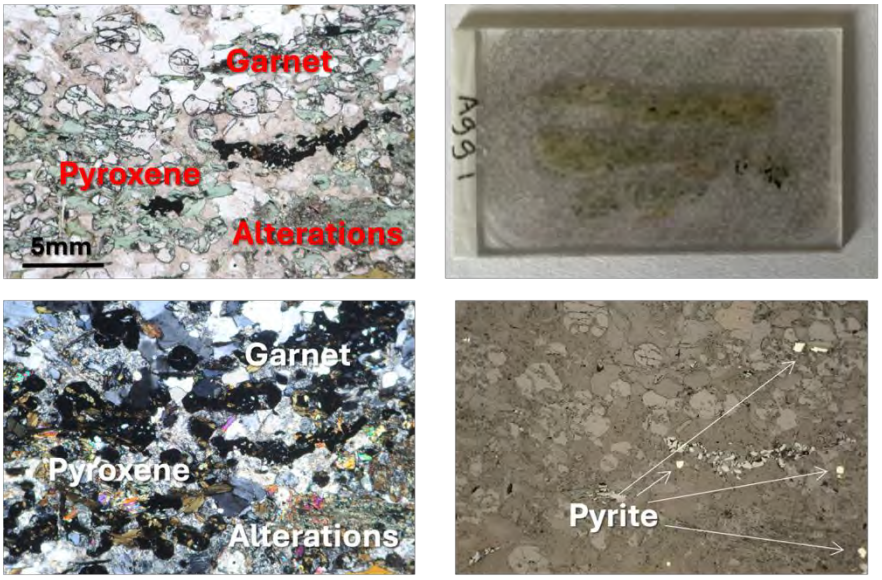

Figure 13. Petrographic images of Aggregate 1. Images taken under transmitted light with (top left) uncrossed polarizers and (bottom left) crossed polarizers and (bottom right) under reflected light.

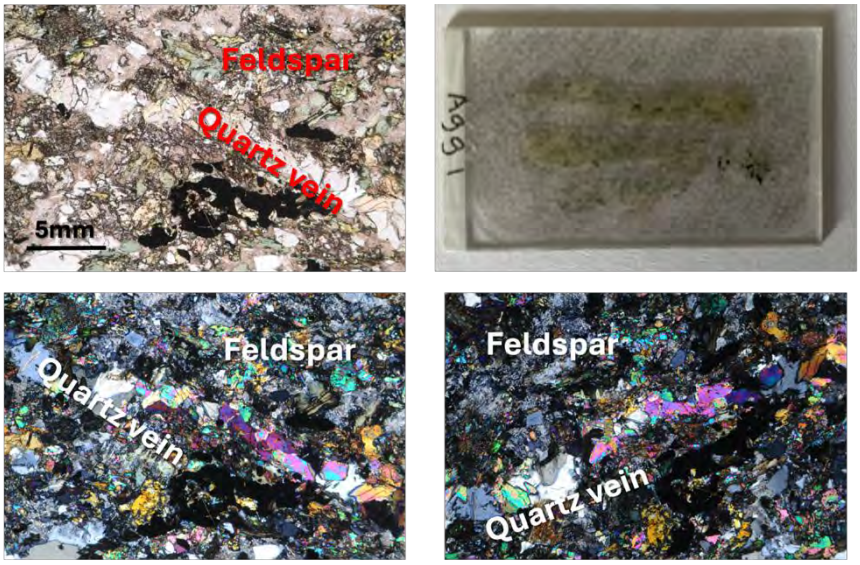

Figure 14. Petrographic images of Aggregate 1 in one of the visible veins. Images taken under transmitted light with (top left) uncrossed polarizers and (bottom left) crossed polarizers and (bottom right) under reflected light.

At a magnification of 5×, Aggregate 2 reveals a mixture of microcline, quartz, and plagioclase, exhibiting a graphic granite texture that suggests it may be an orthoclase mineral. The presence of pink pyroxene and black garnet is noticeable in crossed polarized light, and the green, pink, and blue hues further indicate the orthoclase nature of the specimen (Figure 15). Biotite is also present, and upon rotation in crossed polarized light, hematite–ilmenite and pyrite are observed, with notable amounts of pyroxene throughout the sample. Figure 16 highlights the distinction between garnet and pyroxene, featuring a small amount of pyrite, which appears very bright in reflected light. Further analysis shows green amphibole and brown biotite, although no significant features are observed under higher magnification.

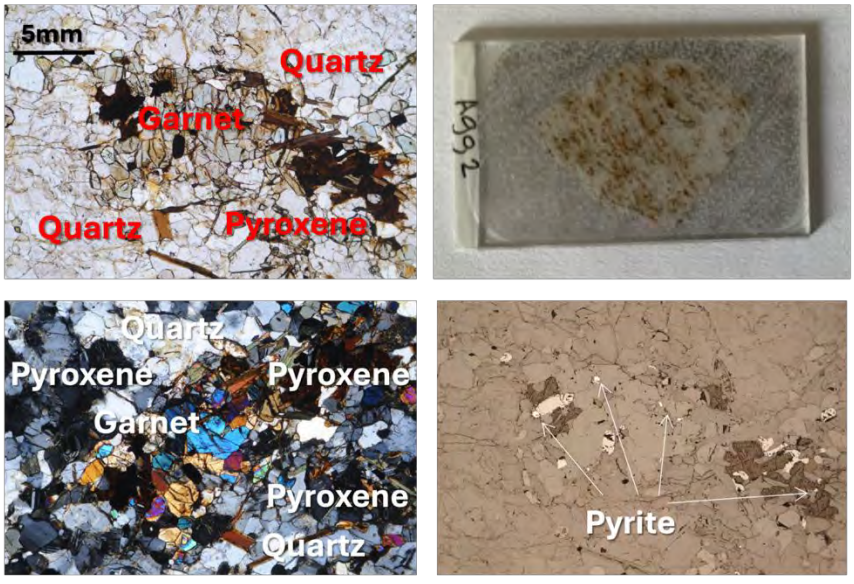

Figure 15. Petrographic images of Aggregate 2. Images taken under transmitted light with (top left) uncrossed polarizers, (bottom left) crossed polarizers, and (bottom right) under reflected light.

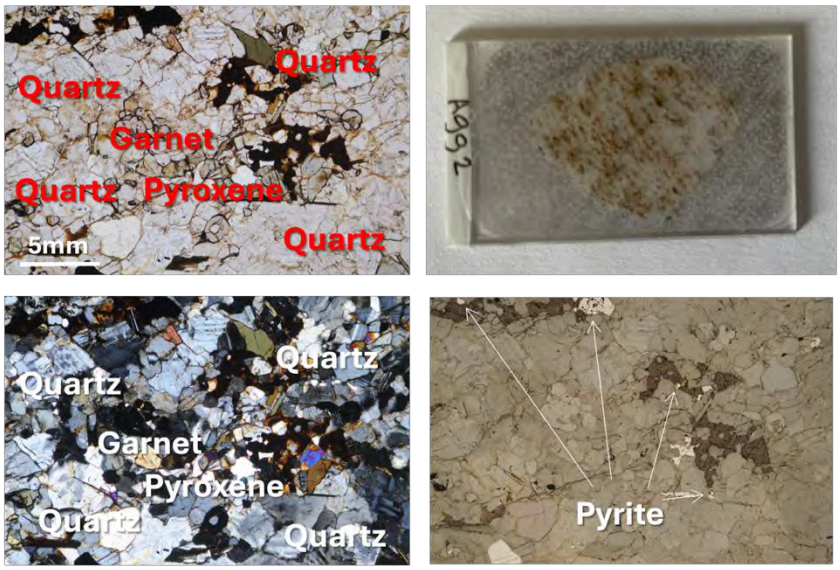

Figure 16. Petrographic images of Aggregate 2, highlighting the distinction between garnet and pyroxene. Images taken under transmitted light with (top left) uncrossed polarizers and (bottom left) crossed polarizers and (bottom right) under reflected light.

3.2.5 Powder XRF of Aggregates

The XRF data are presented in weight percent and normalized to a total of 100%. The analysis cannot detect elements lighter than fluorine. Therefore, any results pertaining to fluorine, sodium, and magnesium should be interpreted with caution because these elements are near the detection threshold of the system and may not be accurately quantified. Table 1 lists the elemental composition of the aggregates, confirming the results discussed in Section 3.2.3. The predominant element in all selected aggregates is silicon, and several samples contain significant amounts of aluminum, potassium, and iron. Aggregates 1 and 3 contain a much higher amount of iron than the other aggregates. The content of calcium also varies among the samples; for the aggregates that contain higher amounts of iron (Aggregates 1 and 3), the calcium content is also significantly higher than the rest (Aggregates 2, 4, and 5).

Table 1. Elemental weight percentages present in Aggregates 1–5 obtained via powder XRF quantitative analysis.

Element	*AGG1*	*AGG2*	*AGG3*	*AGG4*	*AGG5*
	wt %	*wt %*	*wt %*	*wt %*	*wt %*
Mg	5.135	2.331	4.652	1.126	1.022
Al	14.100	13.408	13.383	13.116	12.604
Si	37.351	55.493	36.907	58.843	60.206
P	0.555	0.508	0.678	0.462	0.518
S	0.040	0.000	0.024	0.000	0.000
Cl	0.356	0.399	0.488	0.497	0.516
K	3.492	9.452	4.597	18.572	13.675
Ca	16.492	7.098	14.583	1.539	3.893
Ti	1.577	1.030	1.882	0.721	0.897
V	0.050	0.021	0.048	0.004	0.000
Cr	0.998	0.101	0.053	0.118	0.131
Mn	0.326	0.199	0.389	0.110	0.162
Fe	19.633	9.103	21.635	4.128	5.424
Co	0.216	0.199	0.226	0.167	0.194
Ni	0.170	0.244	0.071	0.236	0.258
Cu	0.033	0.010	0.000	0.008	0.010
Zn	0.031	0.018	0.040	0.012	0.018
Rb	0.019	0.053	0.024	0.075	0.063
Sr	0.152	0.117	0.152	0.084	0.130
Y	0.011	0.009	0.014	0.006	0.009
Zr	0.067	0.100	0.085	0.027	0.099
Nb	0.003	0.005	0.004	0.004	0.006
Mo	0.006	0.013	0.004	0.011	0.012
Ce	0.085	0.089	0.062	0.134	0.154

3.2.6 XRD of Aggregates

Many of the phases observed are monoclinic or triclinic, resulting in numerous overlapping peaks associated with different phases. The presence of preferred orientation within the crystallites introduces further complexity. The interplay of these factors can contribute to increased uncertainty in the quantification of the respective phases. According to this assessment, the aggregates contain the approximate phase percentages shown in Table 2. In accordance with the discussion in Sections 3.2.3 and 3.2.5, based on the phases present in Aggregates 1 and 3, these aggregates can be considered similar. The same can be concluded for Aggregates 2, 4, and 5.

Table 2. Approximate phase percentages in the aggregates obtained by XRD and Rietveld refinement.

Mineral	*Agg 1*	*Agg 2*	*Agg 3*	*Agg 4*	*Agg 5*
Quartz	—	38%	—	30%	35%
Feldspar	57%	44%	43%	33%	35%
Microcline	—	12%	—	33%	25%
Biotite	5%	4%	12%	4%	5%
Hornblende	21%	—	26%	—	—
Diopside	17%	—	6%	—	—

4. OVERVIEW OF STAINLESS STEEL WELDS HARVESTING FROM RINGHALS UNIT 2

Vattenfall has provided access to stainless steel welds extracted from critical piping systems within Ringhals Unit 2. These welds were sourced from the surge line, residual heat removal line, and safety injection line. The majority of the welds are composed of stainless steel 316, fabricated using gas tungsten arc welding and shielded metal arc welding processes. After a series of joint conference calls among representatives from ORNL, NRC, EPRI, Vattenfall, and Studsvik, an agreement was formalized regarding the harvesting and allocation of specific weld samples. Under this agreement, EPRI was designated to harvest one surge line weld, identified as SL3W, while ORNL was tasked with harvesting another surge line weld, identified as SL1W. The NRC has also expressed interest in harvesting an additional stainless steel weld from Ringhals Unit 2 for its own research purposes at a later date.

The SL1W surge line weld has been identified as a key specimen of interest for its relevance to high-priority degradation mechanism studies. Detailed information related to the SL1W weld is provided in Table 3, and Figure 17 illustrates its precise location, geometric layout, and dimensions. The elevated service temperature of the SL1W weld is a critical factor that promotes thermal aging and material embrittlement over time, making it an ideal subject for evaluating the aging effects on stainless steel welds. Of particular interest is the heat-affected zone, where susceptibility to crack initiation increases due to elevated residual stress and microstructural changes induced during welding. Furthermore, the weld will support studies on environmentally assisted fatigue, especially in the weld toe region, which is known to experience high stress concentrations during reactor operation.

Table 3. Information for Ringhals Unit 2 SL1W surge line weld

Component	*Material*	*Welding process*	*Service condition*	*Size*	*Weight*
Surge line weld SL1W half-pipe	Stainless steel 316	Gas tungsten arc welding + Shielded metal arc welding	Turbulent area, 325–335°C	300 × Ø355 mm (180° of circumference)	~110 kg

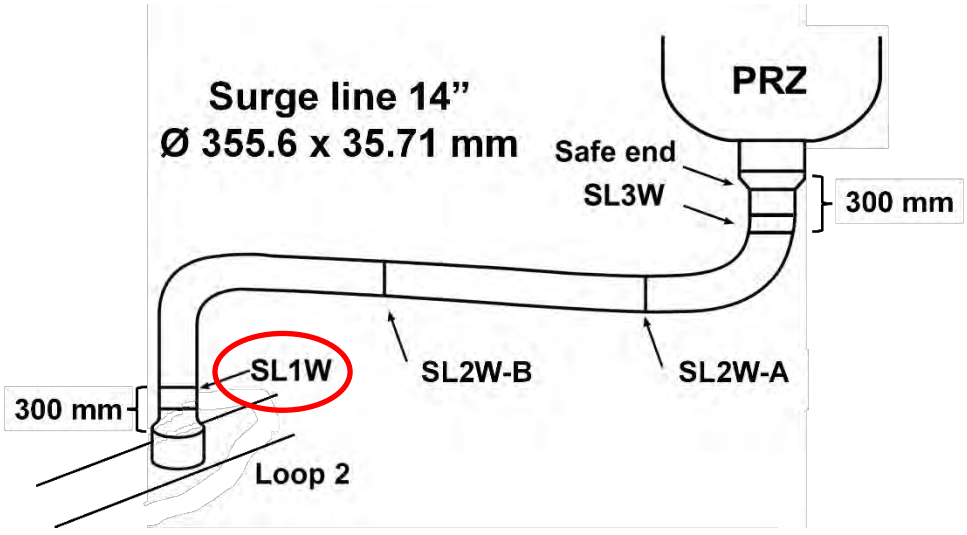

Figure 17. Schematic for the Ringhals Unit 2 surge line welds; PRZ: pressurizer.

To facilitate the removal of the SL1W weld, a subcontract has been initiated with Studsvik, currently the sole entity authorized to harvest metallic components from the Ringhals Units. The subcontract specifies the removal of the SL1W weld, which spans a 180° segment of the surge line. To enhance the utility of the harvested material for various characterization studies while optimizing costs, a formal request has been submitted to Vattenfall for the harvested weld segment to be divided into three equal portions. Two of these portions are to have their interior diameter surfaces ground to eliminate potential contamination and thus provide a non-radioactive material for microstructural and mechanical property evaluations. The third section will remain in its as-harvested condition to enable investigations of early-stage surface degradation and crack initiation under operational conditions.

This division into multiple sections is intended to maximize the breadth of scientific analyses that can be performed on the weld, ranging from thermal aging assessments to fatigue crack growth studies. Additionally, this approach reduces the need for repeated harvesting operations, significantly saving time and resources. The collaborative studies on the SL1W weld will be conducted as part of the LWRS program, with the involvement of ORNL, Argonne, and PNNL. This multidisciplinary effort aims to generate critical data on weld performance under long-term operational conditions, providing insights that will inform strategies for maintaining the structural integrity of aging reactor systems.

5. CONCLUSIONS

This work achieved significant milestones in the characterization of reactor-relevant materials, including unirradiated concrete cores from Ringhals Unit 2 and the SL1W surge-line 316 stainless steel weld. The data generated provide crucial insights into material behavior under operational reactor conditions and contribute to advancing industry efforts to enhance safety margins and extend the service life of aging nuclear reactors.

Key progress was made in the characterization of unirradiated concrete cores. The mineralogy and chemistry of two cores were established, revealing quartz- and feldspar-dominant aggregates with iron-rich inclusions. XCT analysis demonstrated aggregate–matrix heterogeneity, providing insights into crack-path mapping under operational conditions. SEM-EDS automated mineralogy analysis further refined the understanding of the concrete's mineral phases, building a foundation for evaluating mechanical and chemical behavior in future studies.

The opportunity to harvest irradiated concrete from the Ringhals Unit 2 is particularly significant. As some of the first large-scale irradiated concrete samples available for analysis, they will enable direct investigations into radiation-induced changes in mineralogy, microstructure, and mechanical properties. This unprecedented access addresses a critical gap in understanding the long-term durability and performance of reactor safety-critical structures.

Progress on the SL1W surge-line 316 stainless steel weld included its successful acquisition and preparation for detailed analysis. Sectioning and finishing parameters were defined to facilitate microstructural and mechanical evaluations, which are critical steps for future testing. Planning efforts also established a thermal aging test matrix that will assess long-term changes in residual stress distribution, fracture resistance, and structural integrity. These investigations will provide data directly relevant to understanding the performance of metallic components in reactor pressure boundaries under aging and operational stresses.

The baseline data from this work create a foundation for understanding material degradation under combined stress, aging, and irradiation conditions. The results will inform stakeholders about safety margins, material durability, and service-life extensions for nuclear reactor components. Future investigations will leverage the harvested irradiated concrete to examine long-term radiation damage mechanisms and use these insights to validate predictive models that ensure reactor safety and reliability.

REFERENCES

1. Sabatino, S., Le Pape, Y., and Tajuelo Rodriguez, E. (2024). “Concrete Harvesting: Potential Opportunities, Timelines, and Updates for FY 24.” *Technical report* ORNL/SPR-2024/3495. Oak Ridge National Laboratory.
2. Geological Survey of Sweden (SGU). (2024). “SGU's Map Viewer.” https://apps.sgu.se/kartvisare/kartvisare-ballast.html
3. World Nuclear News. (2024). “Nuvia to carry out Ringhals decommissioning work.” https://world-nuclear-news.org/Articles/Nuvia-to-carry-out-Ringhals-decommissioning-work
4. Le Pape, Y., Tajuelo Rodriguez, E., Bran Anleu, P., Brooks, A., Anovitz, L. M., Alpan, A., Sheets, J., Koehler, M., Rother, G., and Rosseel, T. M. (2022). “Assessment of San Onofre Concrete Susceptibility Against Irradiation Damage.” *Research Information Letter Office of Nuclear Regulatory Research* RIL 2022-07.